

Dalton Transactions

Accepted Manuscript



This is an *Accepted Manuscript*, which has been through the Royal Society of Chemistry peer review process and has been accepted for publication.

Accepted Manuscripts are published online shortly after acceptance, before technical editing, formatting and proof reading. Using this free service, authors can make their results available to the community, in citable form, before we publish the edited article. We will replace this *Accepted Manuscript* with the edited and formatted *Advance Article* as soon as it is available.

You can find more information about *Accepted Manuscripts* in the [Information for Authors](#).

Please note that technical editing may introduce minor changes to the text and/or graphics, which may alter content. The journal's standard [Terms & Conditions](#) and the [Ethical guidelines](#) still apply. In no event shall the Royal Society of Chemistry be held responsible for any errors or omissions in this *Accepted Manuscript* or any consequences arising from the use of any information it contains.

ARTICLE

A family of dinuclear lanthanide(III) complexes from the use of a tridentate Schiff base: structural and physical studies, and the case of a Dy^{III}₂ emissive single-molecule magnet[†]

Cite this: DOI: 10.1039/x0xx00000x

Received 00th January 2012,
Accepted 00th January 2012

DOI: 10.1039/x0xx00000x

www.rsc.org/

Nikolaos C. Anastasiadis,^a Dimitris A. Kalofolias,^b Aggelos Philippidis,^c Sofia Tzani,^d Catherine P. Raptopoulou,^d Vassilis Psycharis,^d Constantinos J. Milios,^{*b} Albert Escuer^{*e} and Spyros P. Perlepes^{*a, f}

The use of *N*-salicylidene-*o*-aminophenol (H₂saph) in 4f-metal chemistry has led to the isolation of seven new isostructural lanthanide(III) [Ln^{III}] complexes. More specifically the Ln(NO₃)₃·xH₂O/H₂saph/Et₃N (1:1:1) reaction mixtures in DMF/MeCN gave complexes [Ln₂(NO₃)₂(saph)₂(DMF)₄] (Ln= Sm (**1**); Eu (**2**); Gd (**3**); Tb (**4**); Dy (**5**); Ho (**6**); Er (**7**)) in good yields (~65%). The structures of the isomorphous complexes **3** and **5** were solved by single-crystal, X-ray crystallography; the other complexes are proposed to be isostructural with **3** and **5** based on elemental analyses, IR spectra and powder XRD patterns. The two Ln^{III} atoms in the centrosymmetric molecules of **3** and **5** are doubly bridged by the deprotonated iminophenolato oxygen atoms of two nearly planar η¹:η¹:η²:μ saph²⁻ ligands. The imino nitrogen and five terminal oxygen atoms (the salicylaldimate, two from one bidentate chelating nitrate group and two from two DMF ligands) complete square antiprismatic coordination at each metal centre. The IR spectra of the complexes are discussed in terms of the coordination modes of the ligands present in the complexes. Solid-state emission studies for all **1-7** display identical ligand-based photoluminescence. Dc magnetic susceptibility studies in the 2-300 K range reveal the presence of a weak, intramolecular antiferromagnetic exchange interaction ($J = -0.19(1) \text{ cm}^{-1}$ based on the spin Hamiltonian $H = -J(\hat{S}_{\text{Gd}} \cdot \hat{S}_{\text{Gd}})$) for **3** and probably ferromagnetic exchange interaction within the molecules of **4** and **5**. Ac magnetic susceptibility measurements in zero dc field show temperature- and frequency-dependent out-of-phase signals with two well defined, thermally-activated processes for **5**, suggesting potential single-molecule magnetism character. The U_{eff} value is 17.4 cm⁻¹ for the higher temperature process and 16.2 cm⁻¹ for the lower temperature one. The combination of photoluminescence and single-molecule behaviour in the Dy^{III}₂ complex **5** is critically discussed.

Introduction

Molecular mononuclear, dinuclear, polynuclear (coordination clusters¹) and polymeric (coordination polymers²) lanthanide(III) (Ln^{III}) complexes are a central research theme in inorganic chemistry. Such complexes currently attract the intense interest of synthetic, physical and theoretical chemists due to their involvement in diverse scientific fields/areas, for example Single-Molecule³ and Single-Ion⁴ Magnetism, magnetic refrigeration,⁵ quantum computing,⁶ homogeneous⁷ and heterogeneous⁸ catalysis, optics,⁹ organic transformations,¹⁰

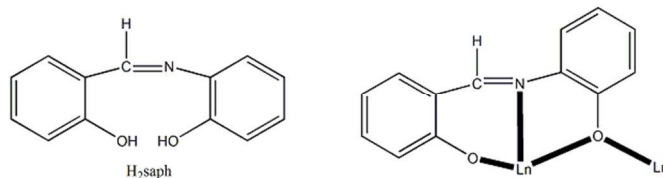
and in the chemistry of multifunctional (or 'hybrid') molecular materials.¹¹ A broad range of applications has been envisioned for Ln^{III}-containing molecules, including use as qubits for quantum information processing,⁶ and prototype devices such as molecular spin valves¹² and transistors.¹³

The creation of multifunctional molecular materials is currently an extremely important challenge in many high-tech applications.¹⁴ Such materials are molecular compounds exhibiting more than one property within the same molecule or family of isomorphous complexes. Dinuclear and polynuclear Ln^{III} complexes are ideal candidates for the construction of

hybrid molecular materials.^{11a,11c,15} Restricting further discussion to the combination of photoluminescent (PL) and Single-Molecule Magnet (SMM) properties, the following features are of key importance. The 4f-4f electronic transitions (responsive for the light emission) are narrow and characteristic of each Ln^{III}, and the emitting excited states are long-lived. To overcome the limitation of the spin- and parity-forbidden nature of 4f-4f transitions, aromatic ligands can be utilized as sensitizers.^{7,16} Highly luminescent Ln^{III} complexes are attracting attention in a wide variety of photonic applications, such as planar waveguide amplifiers, light-emitting diodes and bio-inspired luminescent probes.¹⁷ In the SMM area, some Ln^{III} ions, with their highly anisotropic magnetic moments, have been responsible for many of the recent advances in this interdisciplinary area, pushing the frontiers to longer relaxation times and higher temperature regimes.^{3,18,19} Among the Ln^{III} series, the Dy^{III} member has yielded the largest numbers of 4f-based SMMs,^{3,18} which benefit from both the high magnetic moment and the high anisotropy of the spin-orbit Dy^{III} Kramers doublet ground state ($S=5/2$, $L=5$, $J=15/2$).

Dinuclear Ln^{III} complexes represent one of the simplest units which allow the study of multifunctional Ln^{III} molecular materials, i.e., to investigate the dominance of one property over the other and –within a given property– to answer fundamental questions regarding single-ion behaviour (e.g. magnetic relaxation) *versus* behaviour arising from the molecule as an entity.^{11c,20} Thus Ln^{III}₂ complexes are highly desirable. From the synthetic inorganic chemistry viewpoint, the simplest and most logical route for the isolation of dinuclear 4f-metal ion complexes is the simultaneous employment of bidentate bridging *anionic* groups (e.g. $\eta^1:\eta^1:\mu$ or/and $\eta^1:\eta^2:\mu$ carboxylate groups) and chelating (most often bidentate or tridentate, e.g. bpy, phen, terpy) *neutral* capping organic ligands, which block two or three coordination sites per Ln^{III} ion and terminate further aggregation or potential polymerization.²¹ Another route is the simultaneous employment of capping bidentate nitrate groups and *neutral* or *anionic* organic ligands that bridge the two metal centres.²² Thus, the choice of organic ligands is of paramount importance for the preparation of Ln^{III}₂ complexes.

With all of the above in mind and given the recently initiated interest of our groups in the ‘hybrid’-dual Ln^{III} molecular species, and especially in those displaying both magnetic and electronic-optical properties,²³ we report here the syntheses, structures, magnetism and emission properties of new Ln^{III}₂ complexes, including an emissive Dy^{III}₂ SMM, bearing the tridentate Schiff base *N*-salicylidene-*o*-aminophenol (H₂saph, Scheme 1) as ligand. This Schiff base is a rather well-known ligand in 3d-²⁴ and mixed 3d/4f-metal²⁵ chemistry, but with negligible use²⁶ in homometallic 4f-metal chemistry.



Scheme 1. (left) Structural formula and abbreviation of *N*-salicylidene-*o*-aminophenol, and (right) the coordination mode of its doubly deprotonated form (saph²⁻) in complexes 1-7.

Experimental section

Materials and physical measurements

All manipulations were performed under aerobic conditions using materials (reagent grade) and solvents as received. The organic ligand H₂saph was synthesized in typical yields of >70% following the reported method.²⁷ Its purity was checked by microanalyses and ¹H NMR spectrum. Elemental analyses (C, H, N) were performed by the University of Patras microanalysis service. IR spectra (4000-400 cm⁻¹) were recorded using a Perkin Elmer 16PC FT-IR spectrometer with samples prepared as KBr pellets. Solid-state absorbance spectra were recorded on a Perkin Elmer Lambda 950 UV/VIS spectrometer in the 250-800 nm range, with a step of 2 nm. Solid-state fluorescence spectra were recorded on a Jobin-Yvon Horiba, Fluoro Max-P (SPEX) fluorescence spectrometer with excitation from a cw xenon arc lamp. The slit width for excitation was 1 nm and for emission 5 nm. Powder XRD measurements were collected on freshly prepared samples of the complexes on a PANalytical X'Pert Pro MPD diffractometer. Variable-temperature and variable-field magnetic studies of the Gd(III), Tb(III) and Dy(III) complexes were performed using a DSM5 Quantum Design magnetometer operating at 0.3 T in the 300-30 K range and at 0.02 T in the 30-2.0 K range to avoid saturation effects. Diamagnetic corrections were applied to the observed paramagnetic susceptibility using Pascal's constants.

Synthetic details

Preparation of the representative complex [Gd₂(NO₃)₂(saph)₂(DMF)₄] (3). To a stirred dark yellow solution of H₂saph (0.107 g, 0.5 mmol) and Et₃N (0.067 mL, 0.5 mmol) in a solvent mixture comprising MeCN (5 mL) and DMF (5 mL) was added solid Gd(NO₃)₃·6H₂O (0.226 g, 0.5 mmol). The solid soon dissolved and the resulting yellow solution was stirred for a further 15 min and filtered. The reaction solution was layered with Et₂O (20 mL). Slow mixing gave pale yellow rhombohedral crystals of the product after 4-5 d. The crystals were collected by filtration, washed with MeCN (1 mL) and Et₂O (3x2 mL), and dried in air. The yield was ~65%. Analytical data, calcd for C₃₈H₄₆Gd₂N₈O₁₄ (found values

in parentheses): C 39.57 (39.71), H 4.03 (3.97), N 9.72 (9.56) %. IR bands (KBr, cm^{-1}): 3140w, 3035w, 2930w, 1666s, 1648s, 1606s, 1582m, 1534m, 1480sh, 1466s, 1452sh, 1380s, 1344m, 1324w, 1284s, 1256m, 1244w, 1170m, 1148s, 1106m, 1042w, 1026m, 974w, 916m, 868m, 855sh, 828s, 820sh, 778sh, 760s, 678m, 662m, 598m, 538w, 506sh, 492m, 446w, 410w.

Preparation of complexes $[\text{Ln}_2(\text{NO}_3)_2(\text{saph})_2(\text{DMF})_4]$ (Ln= Sm, **1; Ln= Eu, **2**; Ln= Tb, **4**; Ln= Dy, **5**; Ln= Ho, **6**; Ln= Er, **7**).** These complexes were prepared in an identical manner with **3** by simply replacing $\text{Gd}(\text{NO}_3)_3 \cdot 6\text{H}_2\text{O}$ with the corresponding hydrated nitrate salts of the other lanthanides. Typical yields are in the 60-70% range. The IR spectra of **1**, **2** and **4-7** are almost superimposable with the spectrum of **3** with a maximum wavenumber difference of $\pm 3 \text{ cm}^{-1}$.

Analytical data, calcd for $\text{C}_{38}\text{H}_{46}\text{Ln}_2\text{N}_8\text{O}_{14}$ (found values in parentheses): **1**: C 40.07 (40.28), H 4.08 (3.96), N 9.84 (9.71); **2**: C 39.94 (39.70), H 4.06 (4.00), N 9.81 (9.99); **4**: C 39.46 (39.29), H 4.02 (4.11), N 9.69 (9.50); **5**: C 39.21 (39.37), H 3.99 (4.07), N 9.63 (9.40); **6**: C 39.05 (39.31), H 3.98 (3.87), N 9.59 (9.72); **7**: C 38.89 (39.34), H 3.96 (3.87), N 9.55 (9.80) %.

Single-crystal X-ray crystallography

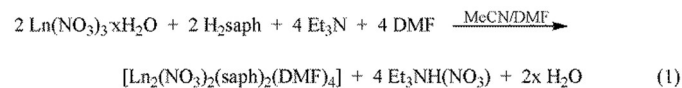
Crystals of **3** (0.22x0.38x0.79 mm) and **5** (0.30x0.35x0.52 mm) were taken from the mother liquor and immediately cooled to -113 °C. Diffraction measurements were performed on a Rigaku R-AXIS SPIDER Image Plate diffractometer using graphite-monochromated $\text{Cu K}\alpha$ radiation. Data collection (ω -scans) and processing (cell refinement, data reduction and Empirical/Numerical absorption correction) were performed using the CrystalClear program package.²⁸ Important crystallographic data are listed in Table S1. The structures were solved by direct methods using SHELXS-97²⁹ and refined by full-matrix least-squares techniques on F^2 with SHELX-97.³⁰ H atoms were either located by difference maps and were refined isotropically or were introduced at calculated positions as riding on their respective bonded atoms. All non-H atoms were refined anisotropically. Full details can be found in the CIF files.

Results and discussion

Syntheses and IR spectra

The reactions of $\text{Ln}(\text{NO}_3)_3 \cdot x\text{H}_2\text{O}$ ($x = 5$ or 6), H_2saph and Et_3N in a 1:1:1 molar ratio in DMF/MeCN (1:1 v/v) gave yellow solutions that upon layering or vapour diffusion with Et_2O gave yellow crystals or crystalline powders of $[\text{Ln}_2(\text{NO}_3)_2(\text{saph})_2(\text{DMF})_4]$ (Ln= Sm (**1**); Eu (**2**); Gd (**3**); Tb (**4**); Dy (**5**); Ho (**6**); Er (**7**)) in good yields (60-70%). The crystals of **3** and **5** were of X-ray quality and their structures were solved by single-crystal X-ray crystallography. The other complexes are proposed to be isostructural with **3** and **5** based on elemental analyses, IR spectra and powder XRD patterns

(Fig. S1). In order to investigate how the reaction's conditions affect the product identity, we tried various metal:ligand: Et_3N ratios (1:1:2, 1:2:2, 1:2:3), but in all cases the same dinuclear complexes were obtained in ~70% yields. Assuming that the dinuclear compounds are the only products from their respective reaction mixtures, the preparation of **1-7** can be represented by eqn (1):



The $\nu(\text{C}=\text{O})$ and $\delta(\text{OCN})$ IR modes of coordinated DMF appear at ~ 1665 , ~ 1650 and $\sim 680 \text{ cm}^{-1}$, respectively, in the spectra of the complexes.³¹ Due to coordination, the $\nu(\text{C}=\text{O})$ and $\delta(\text{OCN})$ bands are shifted to lower and higher wavenumbers, respectively, when compared with the corresponding bands in the spectrum of free DMF.³² The appearance of two $\nu(\text{C}=\text{O})$ bands in the spectra of **1-7** (which is reproducible) probably reflects the presence of two crystallographically independent DMF molecules in the compounds. The spectra of the complexes exhibit strong bands at $1605\text{-}1608 \text{ cm}^{-1}$ which are assigned^{24b,24c} to the $\text{C}=\text{N}$ stretching vibration of the Schiff-base linkage, $\nu(\text{C}=\text{N})$. These bands have been shifted to lower frequencies on going from the free ligand (at 1631 cm^{-1}) to the complexes; this behaviour is typical^{24b} of the coordination of the imino nitrogen to Ln^{III} . The IR bands at ~ 1465 , ~ 1285 and $\sim 1025 \text{ cm}^{-1}$ are assigned³³ to the $\nu_1(A_1)$ [$\nu(\text{N}=\text{O})$], $\nu_3(B_2)$ [$\nu_n(\text{NO}_2)$] and $\nu_2(A_1)$ [$\nu_s(\text{NO}_2)$] vibrational modes of the bidentate chelating (C_{2v}) nitrate group. The separation of the two highest-frequency stretching bands is $\sim 180 \text{ cm}^{-1}$, a typical value for bidentate nitrates.³³

Description of structures

Complexes **3** and **5** are isomorphous and crystallize in the monoclinic space group $P2_1/n$. The molecular structures of the complexes are shown in Figs. 1 and S2. The dinuclear $[\text{Ln}_2(\text{NO}_3)_2(\text{saph})_2(\text{DMF})_4]$ molecules possess an inversion centre at the mid-point of the $\text{Ln1}\cdots\text{Ln1}'$ distance. The two Ln^{III} atoms are doubly bridged by the deprotonated iminophenolato oxygen atoms (O1 , $\text{O1}'$) of two nearly planar, $\eta^1:\eta^1:\eta^2:\mu$ saph²⁻ ligands, the $\text{Ln}^{\text{III}}\cdots\text{Ln}^{\text{III}}$ distance being 3.784 and 3.738 Å for **3** and **5**, respectively. The imino nitrogen and five terminal oxygen atoms (the salicylaldiminate, two from one asymmetric bidentate chelating nitrate group and two from two DMF molecules) complete 8-coordination at each metal site. The Dy-O/N bond lengths are slightly shorter than the corresponding Gd-O/N ones due to lanthanide contraction. A SHAPE analysis³⁴ reveals that the coordination geometry of the 8-coordinate Ln^{III} centres is square antiprismatic (Figs. 2 and S3-S5, Table S2). The two square bases consist of atoms O1 , $\text{O1}'$, O2 , N1 and O3 , O4 , O6 , O7 ; the angle between the best mean planes of the square bases is 2.1° for **3** and 1.7° for **5**. The square antiprism, along with the bicapped trigonal prism and the triangular dodecahedron seem to be the most common

polyhedra among 8-coordinate complexes³⁵ and were termed by Muetterties and Wright ‘low energy polyhedra’.³⁶

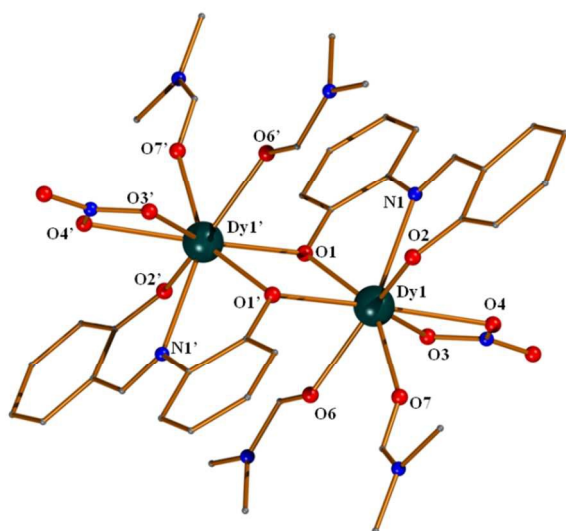


Fig. 1 The molecular structure of **5**. Unprimed and primed atoms are related by the symmetry operation $-x+2, -y, -z$. Selected interatomic distances (Å) and angles ($^{\circ}$): Dy1...Dy1' 3.738(1), Dy1-O1 2.323(2), Dy1-O1' 2.322(3), Dy1-O2 2.200(3), Dy1-N1 2.525(4), Dy1-O(NO₃⁻, DMF) 2.319(3)-2.482(3) Å; O1-Dy1-O1' 72.8(1), O3-Dy1-O4 51.7(1), O1'-Dy1-O4 163.3(1), O2-Dy1-O6 146.9(1), Dy1-O1-Dy1' 107.2(1) $^{\circ}$. Colour scheme: Dy, dark green; N, blue; O, red; C, grey.

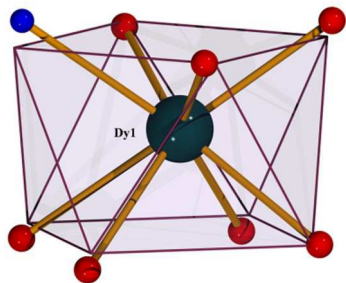


Fig. 2 The square antiprismatic coordination geometry of Dy1 in the structure of **5**. The plotted polyhedron is the ideal, best-fit polyhedron using the program SHAPE.³⁴

The lattice structures of the two complexes are built through weak intermolecular C-H...O interactions involving one aromatic carbon atom of the iminophenolate part of saph²⁻ and one coordinated nitrate oxygen atom. The dinuclear molecules form 2D layers extending parallel to the (101) plane (Figs. 3 and S6).

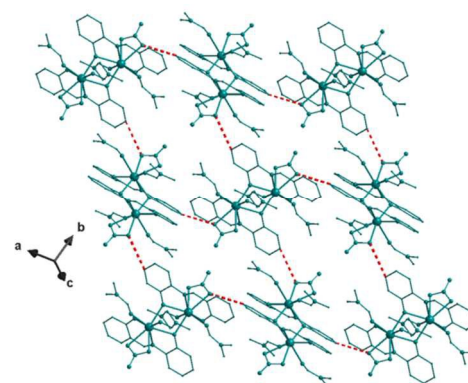


Fig. 3 A small portion of one 2D layer in the crystal structure of complex **5**, resulting from the intermolecular C3-H3...O4 (and symmetry equivalent) hydrogen bonding interaction.

Complexes **3** and **5** join a very small family of structurally characterized Ln^{III}-containing complexes that possess anionic forms of H₂saph as ligands. Four of them are 3d/4f-metal complexes²⁵ and only compound [Dy₆(OH)₂(O₂CMe)(Hsaph)(saph)₇(H₂O)(MeOH)₂]²⁶ is a pure 4f-metal cluster. Since all these complexes were reported only recently, we feel it timely to collect them in Table 1 together with the coordination modes of saph²⁻ and Hsaph⁻, and basic information about their magnetic behaviour. Thus, complexes **3** and **5** are the first dinuclear Ln^{III} complexes of saph²⁻/Hsaph⁻.

Table 1 Structurally characterized Ln^{III}-containing complexes that possess Hsaph⁻ and saph²⁻ as ligands

Complex	Coordination mode	Magnetic Behaviour ^{b,c}	Ref.
(Et ₃ NH)[Mn ^{III} ₄ Dy ₃ O ₂ (OH) ₄ (NO ₃) ₄ (saph) ₈ (H ₂ O) ₄]	$\eta^1-\eta^1-\eta^2-\mu_3$	AF, SMM	25a
[Mn ^{III} ₄ Dy ₃ O ₂ (OH)(NO ₃) ₃ (Hsaph)(saph) ₆ (H ₂ O)]	$\eta^1-\eta^2-\mu_3^a$ $\eta^1-\eta^1-\eta^2-\mu_3$	AF/F, SMM	25a
[Ni ₅ Gd ₃ (OH) ₅ (OMe)(O ₂ CPh) ₃ (saph) ₅ (MeOH) ₄ (H ₂ O)]	$\eta^2-\eta^1-\eta^2-\mu_3$ $\eta^2-\eta^1-\eta^2-\mu_3$	F	25b
[Ni ₅ Dy ₃ (OH) ₅ (OMe)(O ₂ CPh) ₃ (saph) ₅ (MeOH) ₄ (H ₂ O)]	$\eta^2-\eta^1-\eta^2-\mu_3$ $\eta^3-\eta^1-\eta^1-\mu_3$	AF, SMM	25b
[Dy ₆ (OH) ₂ (O ₂ CMe)(Hsaph)(saph) ₇ (MeOH) ₂ (H ₂ O)]	$\eta^1-\eta^1-\eta^1^a$ $\eta^1-\eta^1-\eta^2-\mu$	AF, SMM	26
[Gd ₂ (NO ₃) ₂ (saph) ₂ (DMF) ₄] (3)	$\eta^1-\eta^1-\eta^2-\mu$	AF	this work
[Dy ₂ (NO ₃) ₂ (saph) ₂ (DMF) ₄] (5)	$\eta^1-\eta^1-\eta^2-\mu$	F, SMM	this work

^a For the Hsaph⁻ ligand. ^b AF= overall antiferromagnetic behaviour, F= overall ferromagnetic behaviour, SMM= Single-Molecule Magnet. ^c The assignment of AF or/and F exchange interactions in the 3d/Dy^{III} and Dy^{III} complexes should be considered as tentative and taken into account with skepticism.

Absorption and emission spectra

The solid-state electronic absorption spectra of all complexes were recorded; the spectra of the representative complexes **4** and **5**, as well as the spectrum of H₂saph are shown in Fig. S7. The spectra of **1-7** are very similar, dominated by ligand-based bands. Due to deprotonation and coordination, the absorption bands of free H₂saph at 454 and 486 nm are ‘‘blue’’ shifted by ca. 90 and 80 nm, respectively, in the spectra of the complexes. In accordance with the fact that deprotonation causes ‘‘blue’’ shift, a methanolic solution of H₂saph containing 2.5 equivalents of LiOH (assumed to contain a high concentration

of saph^{2-}) exhibits the two longest wavelength absorptions at 420 and 445 nm.

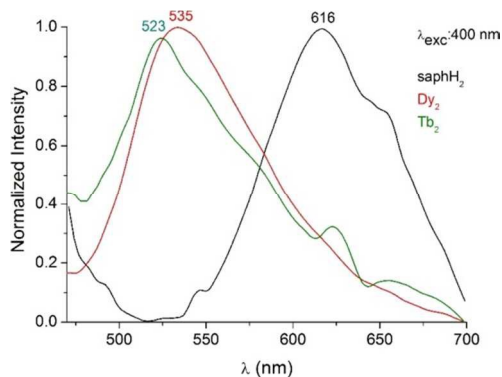


Fig. 4 Solid-state, room-temperature emission spectra for the neutral H_2saph , and complexes **4** and **5** that contain the doubly deprotonated (saph^{2-}) form of the ligand. The excitation wavelength was 400 nm in all cases.

Solid-state, room-temperature emission spectra of the free ligand H_2saph and complexes **4** and **5** are presented in Fig. 4. Upon maximum excitation at 400 nm, a strong emission peak at 616 nm and a shoulder at *ca.* 650 nm are detected for free solid H_2saph . This spectral pattern remains the same upon excitation at 485 and 450 nm (Fig. S8). Since solid “salts” $\text{A}_2(\text{saph})$, where $\text{A}^+ = \text{Li}^+, \text{Na}^+, \text{K}^+, \text{Et}_3\text{NH}^+, \text{Bu}^n\text{N}^+, \dots$, are not known in the literature (our efforts to prepare such “salts” repeatedly failed leading to mixture of products difficult to separate and characterize), we were not able to compare the solid-state emission spectra of the complexes with the corresponding spectrum of the free saph^{2-} ion. However, a methanolic “ $\text{H}_2\text{saph} + 2.5\text{LiOH}$ ” solution emits weakly green light displaying a broad peak at *ca.* 550 nm upon excitation at 400 nm. An almost identical, room-temperature photoluminescence behaviour is observed for solids **1-7** (Fig. 4 for **4** and **5**, Fig. S9 for **1**). Upon maximum excitation at 400 nm, a broad green emission at *ca.* 530 nm was recorded; no significant Ln^{III} emission ($\text{Ln} = \text{Sm}, \text{Eu}, \text{Tb}, \text{Dy}$) was detected. These experimental facts reveal²³ that the broad green emission at ~ 530 nm in the spectra of all complexes is saph^{2-} -centered.

Dc magnetic susceptibility studies

Solid-state direct-current (dc) magnetic susceptibility (χ_M) data on powder samples of complexes **3**, **4** and **5** were collected under applied fields of 0.3 T (300-30 K) and 0.02 T (30-2.0 K). The data are plotted as $\chi_M T$ products *versus* T in Fig. 5. The room-temperature $\chi_M T$ value for **3** is $16.01 \text{ cm}^3 \text{ K mol}^{-1}$, essentially equal to the spin-only value ($15.75 \text{ cm}^3 \text{ K mol}^{-1}$ for $g = 2.00$) expected for two noninteracting Gd^{III} ($S = 7/2, L = 0$) ions. The value of the $\chi_M T$ product remains almost constant down to ~ 30 K and then decreases rapidly to $6.59 \text{ cm}^3 \text{ K mol}^{-1}$ at 2.0 K, suggesting a moderately weak antiferromagnetic exchange interaction. Fit of the experimental data was performed by means of the conventional analytical expression derived from the isotropic spin Hamiltonian shown in eqn (2). The best-fit parameters obtained are $J = -0.19(1) \text{ cm}^{-1}$ and $g = 2.023(1)$. The J value is typical for dinuclear complexes containing the $\{\text{Gd}^{\text{III}}_2(\mu\text{-OR})_2\}$ core.^{3,13a,37,38}

$$H = -J(\hat{S}_{\text{Gd}} \cdot \hat{S}_{\text{Gd}}) \quad (2)$$

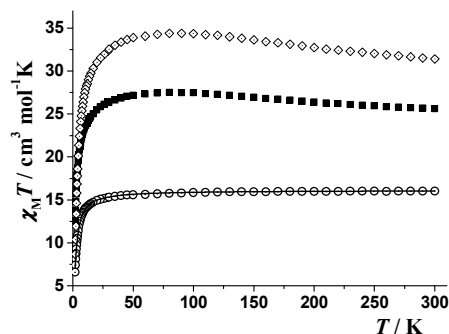


Fig. 5 $\chi_M T$ versus T plots of complexes **3** (open circles), **4** (solid squares) and **5** (diamonds); the solid line is the fit of the data to the theoretical model for the Gd^{III}_2 complex; see the text for the fit parameters.

Magnetization measurements for the Gd_2 complex **3** show a slightly sigmoid shape with a saturation value of 14.1 electrons under an applied field of 5 T, corresponding to the expected value for two weakly coupled Gd^{III} ions.

The room-temperature $\chi_M T$ values for **4** and **5** (25.60 and $31.40 \text{ cm}^3 \text{ K mol}^{-1}$, respectively) are in agreement with the expected values of 23.64 and $28.34 \text{ cm}^3 \text{ K mol}^{-1}$ for two noninteracting Tb^{III} (7F_6 , free ion; $S = 3; L = 3; g_J = 3/2$) and Dy^{III} (${}^6H_{15/2}$, free ion; $S = 5/2; L = 5; g_J = 4/3$) centres, respectively. Upon cooling, the values of the $\chi_M T$ product for both complexes increase up to maximum values of 27.50 (**4**) and 34.38 (**5**) $\text{cm}^3 \text{ K mol}^{-1}$ at *ca.* 80 K. Below this temperature, the $\chi_M T$ values decrease continuously down to 12.60 (**4**) and 8.68 (**5**) $\text{cm}^3 \text{ K mol}^{-1}$ at 2.0 K. The increase of $\chi_M T$ in the 300-80 K range *might* indicate moderate intramolecular ferromagnetic $\text{Tb}^{\text{III}} \dots \text{Tb}^{\text{III}}$ and $\text{Dy}^{\text{III}} \dots \text{Dy}^{\text{III}}$ exchange interactions. It should be explicitly mentioned at this point that the profiles of $\chi_M T$ *versus* T curves on Ln^{III} complexes other than Gd^{III} cannot be assigned to ferro- or antiferromagnetic coupling.³⁹ Such wrong assignments appear sometimes in experimental reports without a deep analysis of the data.⁴⁰ The spin Hamiltonian works only for Gd^{III} , the other lanthanides(III) needing much more complex models, based on explicit ligand field spin-orbit parameters.^{39,40} Usually such treatments are not carried out, a situation excusable by their complexity (a multitude of parameter which usually cannot be solved with respect to available experimental data). The decrease below 80 K can be attributed mainly to the depopulation of the Tb^{III} and Dy^{III} m_J sublevels of the ground J state, with the possibility of intermolecular antiferromagnetic exchange/dipolar interactions also contributing to this behaviour.¹⁹ The gradual increase of the $\chi_M T$ values upon cooling in the 300-80 K range might suggest the orientation of the microcrystals of the samples in the magnetic field.⁴⁰ We should state at this point that the measurements were twice (thus they are reproducible) performed for each compound on powdered, but well compacted, samples in a manner which avoids rotation of the microcrystals; so, we are sure that our experimental method is correct. On the other hand, rotation of the crystalline samples during the measurements could be important at low temperatures, but a moderate field of 0.3 T can not justify the $\chi_M T$ increase upon cooling in the ‘high’ temperature region (300-80 K). Moreover, the magnetization increases rapidly probably suggesting ferromagnetic compounds, without any anomalous change of slope. In addition, the ac $\chi'_M T$ values

under an external field of 4 G agree with the low- T $\chi_M T$ values at higher fields (145 and 3000 G); orientation of the crystals under a field of 4 G can be ruled out.

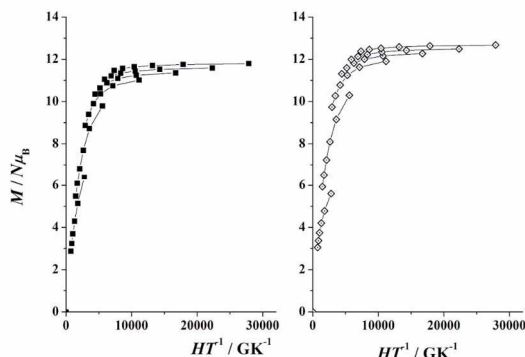


Fig. 6 Reduced magnetization plots for compounds **4** (left) and **5** (right) at low temperatures. The solid lines are guides for the eye.

The lack of a superposition of the reduced magnetization (M) versus H/T data on a single master curve and the low magnetizations of $11.9 N\beta$ for **4** and $12.8 N\beta$ for **5** at 5 T (Fig. 6) suggest the presence of a moderate magnetic anisotropy and/or low-lying excited states.

Ac magnetic susceptibility studies

In the light of the dc susceptibility measurements and magnetization responses, alternating-current (ac) magnetic susceptibility measurements were performed on polycrystalline samples of **4** and **5** in the 2.0-12 K range in zero applied dc field and a 4.0 G ac field oscillating in the 10-1488 Hz range (Figs. 7 and S10). No out-of-phase (χ''_M) signals were detected for **4**, but well defined frequency-dependent χ''_M signals were observed for **5**, indicative of SMM behaviour. The χ''_M ac signals show two peaks corresponding to two well defined, thermally-activated processes around 6 K for frequencies in the

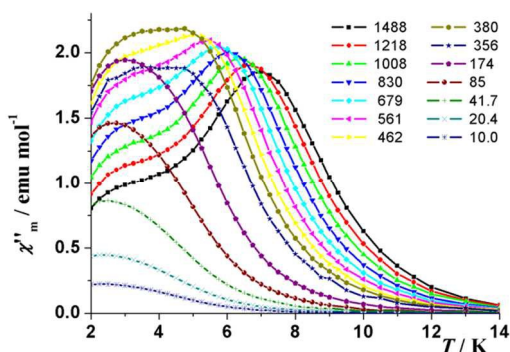


Fig. 7 Out-of-phase (χ''_M) versus T ac magnetic susceptibility signals for **5** in a 4.0 G ac field oscillating between 1488 and 10 Hz; solid lines are guides for the eye and frequencies are given in Hz.

1488-561 Hz range and around 2.5 K for frequencies ranging between 174 and 10 Hz. At intermediate frequencies (462, 380, 356 Hz), the peaks overlap and the position of the maxima are not clearly defined.

Fitting to the Arrhenius law [$\tau = \tau_0 \exp(U_{\text{eff}}/K_B T)$] (Fig. 8) afforded values of $U_{\text{eff}} = 17.4 \text{ cm}^{-1}$ and $\tau_0 = 3.0 \times 10^{-6} \text{ s}$ for the process at $\sim 6 \text{ K}$, and $U_{\text{eff}} = 16.2 \text{ cm}^{-1}$ and $\tau_0 = 4.4 \times 10^{-7} \text{ s}$ for the lower temperature process. As expected, the flattened (i.e. non-semicircular shape) Cole-Cole plot at 5 K (Fig. 9) confirms⁴¹ the two simultaneous relaxation processes. The relaxation time, τ , does not become temperature independent even down to 2.2 K, indicating that a pure quantum regime is not yet active.

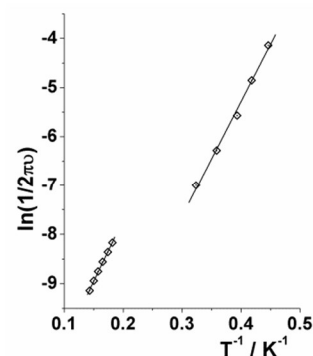


Fig. 8 Plots of $\ln(\tau)$ versus T^{-1} for **5** under a zero applied dc field in the frequency ranges 1488-561 and 174-10 Hz. The solid lines represent the fits to the Arrhenius equation.

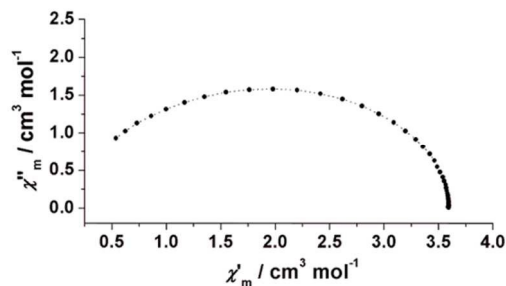


Fig. 9 Cole-Cole (Argand) plot for **5** obtained using the ac susceptibility data at 5 K; the frequencies range from 1 Hz (highest χ'_M) up to 1488 Hz (lowest χ'_M). The dotted line is a guide for the eye.

The observation of more than one relaxation process in Dy^{III}_2 units has been related either with the presence of two different metal sites in the molecule or with relaxation of the ground state through excited levels.^{3,19e,42} Since complex **5** is centrosymmetric with a unique metal site, the latter possibility emerges as the reasonable origin of the two processes. The topic of magnetic relaxation in Ln(III) SMMs is of great current interest.^{3b,18c,19e,40b,43} Magnetic relaxation is typically controlled by single-ion factors rather than magnetic exchange and proceeds through thermal relaxation of the lowest excited states. For a Kramers doublet Ln^{III} (like Dy^{III}) SMM, the lowest energy doublet has high $|m_j|$, and the complexity of the relaxation phenomena is related to the number of relaxation paths available (reversal mechanism via quantum tunnelling of magnetization within the lowest energy doublet, thermal mechanism via an excited state, thermally activated quantum

tunnelling of magnetization occurring within an excited doublet).

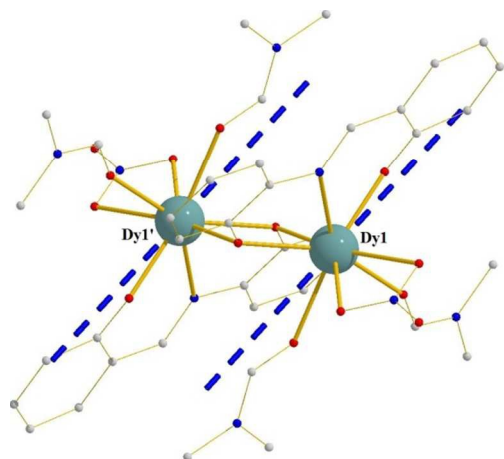


Fig. 10 Ground state magnetic anisotropy axes for the two Dy ions present in **5**.⁴³

Given that in the absence of high symmetry, the ground state of Dy^{III} is a doublet quantized along the anisotropy axis with $m_j = \pm 15/2$, we have determined the orientation of the ground state magnetic anisotropy axis for each Dy^{III} centre of **5** using a method reported recently, based on an electrostatic model.⁴⁴ The method does not rely on the fitting of experimental data, requiring only the determination of the single-crystal X-ray structure of the complex. Following this method and the program MAGELLAN (a FORTRAN program), the ground state magnetic axis for each Dy^{III} ion in **5** (the two axes are co-parallel due to the presence of a crystallographically imposed inversion centre in the molecule) was found tilted towards the DMF atom O7 and the terminal oxygen atom O2 which belongs to the salicylidene part of saph²⁻ (Fig. 10), i.e. pointing toward the square faces of the approximate antiprism. However, after several decades of studies on ligand field theories, it is well established that the electrostatic models are not completely valid neither for lanthanide nor for transition metal complexes.⁴⁵ Thus, although this electrostatic model gives probably a good orientation, it should be treated with caution due to its limitations.

Conclusions and perspectives

In this report, we have shown that the dianion of *N*-salicylidene-*o*-aminophenol can act as a ligand support for seven isostructural Ln^{III}₂ complexes (Ln = Sm, Eu, Gd, Tb, Dy, Ho, Er). All complexes studied exhibit intense, ligand-based emission. The Tb^{III} and Dy^{III} compounds display weak ferromagnetic exchange; in addition, the Dy^{III}₂ complex shows SMM behaviour at low temperatures with two relaxation processes. Thus, SMM and emissive behaviours are observed in the same molecule.

The design of lanthanide multifunctional materials is one of the most challenging themes in the field of molecular materials

science. One of the attractive targets is the preparation of complexes containing both SMM and Ln^{III}-based emission properties,^{11,15} and our groups have been trying to isolate and characterize such compounds.¹⁴ The combination of these properties would, for example, permit the comparison of the energy gap between the ground state and the first excited state using two techniques (ac fit and luminescence spectrum), as carried out in an excellent way for a redox-active, near-IR luminescent Yb^{III}₂ SMM.^{11c} In the case of **5**, the observed green emission is not due to Dy^{III}. A first, albeit simplistic, explanation could be that Dy^{III} normally emits in approximately the same spectral region (blue, blue-green) with that of free saph²⁻ (green), and its emission is overlapped and thus is not detectable. However, the fact that all solid complexes **1-7** display an identical room-temperature photoluminescence (e.g. it is well known that Eu^{III} emits in the red region and emission would be expected in the present case), indicates that there is no efficient energy transfer “sensitization” of the Ln^{III} ion’s excited levels from the ligand’s triplet state.¹⁷ A reason for this could be the fact that the main absorption bands of H₂saph/saph²⁻ (>400 nm) are not close to the region where some Ln^{III} ions absorb (<400 nm). This means that the ligand(singlet state)→ligand(triplet state)→Ln* energy flow has to be optimized by adjusting the energy gap between the lowest ligand triplet state and the Ln^{III} emitting levels; this requires a change of the ligand. It should be mentioned at this point that although the above mentioned energy flow appears simple (and often discussed and modelled as simple), sensitization of Ln^{III} ions is an exceedingly complex process involving numerous rate constants and its fine-tuning requires the adjustment of several parameters.⁴⁶

We are currently investigating the possible presence of a second family of products in the Ln(NO₃)₃·xH₂O/H₂saph general reaction system. Work also is in progress to enhance the aromatic content of the present complexes, e.g. by adding phenyl rings to the H₂saph backbone and/or using PhCO₂⁻ instead of NO₃⁻ groups, with the hopes to alter the emission properties of the Schiff-base ligand, to achieve efficient energy transfer from the ligand moiety to the lanthanide and “switch on” Ln^{III}-based emission, while retaining the SMM property for the Dy^{III} (and/or Tb^{III}) complexes. Finally, we are searching other means^{46,47} for exciting the Ln^{III} ions in the Ln^{III}/saph²⁻ (and substituted derivatives) family of complexes, i.e. by taking advantages of the ligand-to-metal charge-transfer states (for Sm^{III} and Eu^{III}), a fact that requires carefully designed modification of the ligands, and by using d-transition metal ions as activators of the Ln^{III} luminescence, a fact that requires the synthesis of heterometallic d/4f/saph²⁻ (and substituted derivatives) complexes.

Acknowledgements

This work was supported by the ARISTEIA Action (Project code 84, acronym MAGCLOPT) of the Operational Programme “Education and Lifelong Learning”, co-funded by ESF and

National Resources (to S.P.P.), and by the CICYT (project CTQ2012-30662) and Excellence in Research ICREA-Academic Award (to A.E.).

Notes and references

^a Department of Chemistry, University of Patras, 265 04 Patras, Greece.

E-mail: perlepes@patreas.upatras.gr; Tel: +30 2610 996730

^b Department of Chemistry, University of Crete, Voutes, 710 03 Herakleion, Greece. E-mail: kamil@chemistry.uoc.gr; Tel: +30 2810 545099

^c Institute of Electronic Structure and Laser, Foundation for Research and Technology- Hellas (IESL-FORTH), P.O. Box 1385, 711 10 Herakleion, Greece.

^d Institute of Nanoscience and Nanotechnology, NCSR "Demokritos", 153 10 Aghia Paraskevi Attikis, Greece.

^e Departament de Química Inorganica, Universitat de Barcelona, Diagonal 645, 08028 Barcelona, Spain. E-mail: albert.escuer@ub.edu; Tel: +34 93 4039138

^f Institute of Chemical Engineering Sciences, Foundation for Research and Technology-Hellas (FORTH/ICE-HT), Platani, P.O. Box 1414, 265 04 Patras, Greece.

† Electronic Supplementary Information (ESI) available: Powder XRD patterns (Fig. S1), additional structural (Figs. S2-S6), optical (Figs. S7-S9) and magnetic (Fig. S10) plots, as well as a table with important crystallographic data for complexes **3** and **5** (Table S1) and a table with Continuous Shape Measures (CShM) values for the possible coordination polyhedra of the 8-coordinate Ln^{III} atoms in the molecular structures of **3** and **5** (Table S2). CCDC 1039917 (complex **1**) and 1039918 (complex **2**). For ESI and crystallographic data in CIF or other electronic format see DOI: 10.1039/c000000x/

- G. E. Kostakis, A. M. Ako and A. K. Powell, *Chem. Soc. Rev.*, 2010, **39**, 2238.
- The first use of the term "coordination polymer" may be found in: J. C. Bailar, Jr., in *Preparative Inorganic Chemistry*, ed. W. L. Jolly, Interscience, New York, 1964, vol. 1, pp. 1-25.
- For excellent reviews, see: (a) D. N. Woodruff, R. E. P. Winpenny and R. A. Layfield, *Chem. Rev.*, 2013, **113**, 5110; (b) P. Zhang, L. Zhang and J. Tang, *Dalton Trans.*, 2015, **44**, 3923.
- (a) J. Luzon and R. Sessoli, *Dalton Trans.*, 2012, **41**, 13556; (b) H. L. C. Feltham, Y. Lan, F. Klöwer, L. Ungur, L. F. Chibotaru, A. K. Powell and S. Brooker, *Chem. Eur. J.*, 2011, **17**, 4362; (c) J.-L. Liu, Y.-C. Chen, Y.-Z. Zheng, W.-Q. Lin, L. Ungur, W. Wernsdorfer, L. F. Chibotaru and M. -L. Tong, *Chem. Sci.*, 2013, **4**, 3310; (d) M. Ren, D. Pinkowicz, M. Yoon, K. Kim, L.-M. Zheng, B. K. Breedlove and M. Yamashita, *Inorg. Chem.*, 2013, **52**, 8342; (e) S. Nayak, G. Novitchi, M. Holynska and S. Dehnen, *Eur. J. Inorg. Chem.*, 2014, 3065; (f) N. Ishikawa, M. Sugita, T. Ishikawa, S. Koshihara and Y. Kaizu, *J. Am. Chem. Soc.*, 2003, **125**, 8694; (g) S. D. Jiang, B. W. Wang, G. Su, Z. M. Wang and S. Gao, *Angew. Chem. Int. Ed.*, 2010, **49**, 7448.
- (a) T.-Z. Zheng, G.-J. Zhou, Z. Zheng and R. E. P. Winpenny, *Chem. Soc. Rev.*, 2014, **43**, 1462; (b) J.-L. Liu, Y.-C. Chen, F.-S. Guo and M.-L. Tong, *Coord. Chem. Rev.*, 2014, **281**, 26; (c) R. Sessoli, *Angew. Chem., Int. Ed.*, 2012, **51**, 43; (d) M. Evangelisti, O. Roubeau, E. Palacios, A. Camón, T. N. Hooper, E. K. Brechin and J. J. Alonso, *Angew. Chem., Int. Ed.*, 2011, **50**, 6606; (e) J. W. Sharples, D. Collison, E. J. L. McInnes, J. Schnack, E. Palacios and M. Evangelisti, *Nature Commun.*, 2014, **5**, 5321.
- (a) G. Aromi, D. Aguila, P. Gamez, F. Luis and O. Roubeau, *Chem. Soc. Rev.*, 2012, **41**, 537; (b) F. Luis, A. Repollés, M. J. Martínez-Pérez, D. Aguila, O. Roubeau, D. Zueco, P. J. Alonso, M. Evangelisti, A. Camón, J. Sesé, L. A. Barrios and G. Aromi, *Phys. Rev. Lett.*, 2011, **107**, 117203; (c) M. J. Martínez-Pérez, S. Cardona-Serra, C. Schlegel, F. Moro, P. J. Alonso, H. Prima-García, J.-M. Clemente-Juan, M. Evangelisti, A. Gaita-Arino, J. Sesé, J. van Slageren, E. Coronado and F. Luis, *Phys. Rev. Lett.*, 2012, **108**, 247213.
- (a) S. A. Schuetz, E. A. Bowman, C. M. Silvernail, V. M. Day and J. A. Belot, *J. Organomet. Chem.*, 2005, **690**, 1011; (b) G. K. Veits and J. Read de Alaniz, *Tetrahedron*, 2012, **68**, 2015.
- R. Sen, D. K. Harza, S. Koner, M. Helliwell, M. Mukherjee and A. Bhattacharjee, *Polyhedron*, 2010, **29**, 3183.
- (a) J.-C. G. Bunzli, *Acc. Chem. Res.*, 2006, **39**, 53; (b) S. Swavey and R. Swavey, *Coord. Chem. Rev.*, 2009, **253**, 2627; (c) G. Zucchi, O. Maury, P. Thuery and M. Ephritikhine, *Inorg. Chem.*, 2008, **47**, 10398.
- For example, see: B. Hussain, D. Savard, T. J. Burchell, W. Wernsdorfer and M. Murugesu, *Chem. Commun.*, 2009, 1100.
- (a) D. I. Alexandropoulos, S. Mukherjee, C. Papatriantafyllopoulou, C. P. Raptopoulou, V. Psycharis, V. Bekiari, G. Christou and Th. C. Stamatatos, *Inorg. Chem.*, 2011, **50**, 11276; (b) S. Goswami, A. Adhikary, H. S. Jena and S. Konar, *Dalton Trans.*, 2013, **42**, 9813; (c) F. Pointilart, B. Le Guennic, S. Golhen, O. Cador, O. Maury and L. Quahab, *Chem. Commun.*, 2013, **49**, 615.
- M. Urdampilleta, S. Klyatskaya, J.-P. Cleuziou, M. Ruben and W. Wernsdorfer, *Nature Mater.*, 2011, **10**, 502.
- R. Vincent, S. Klyatskaya, M. Ruben, W. Wernsdorfer and F. Balestro, *Nature*, 2012, **488**, 357.
- (a) P. Gömer-Romero and C. Sanchez, *Functional Hybrid Materials*, Wiley-VCH, Weinheim, Germany, 2004; (b) *Multifunctional Molecular Materials*, ed. L. Quahab, Pan Stanford Publishing Pte. Ltd., Singapore, 2013; (c) H. Hiraga, H. Miyasaka, K. Nakata, T. Kajiwara, S. Takaishi, Y. Oshima, H. Nojiri and M. Yamashita, *Inorg. Chem.*, 2007, **46**, 9661.
- (a) T. Kajiwara, M. Hasegawa, A. Ishii, K. Katagiri, M. Baatar, S. Takaishi, N. Iki and M. Yamashita, *Eur. J. Inorg. Chem.*, 2008, 5565; (b) E. C. Mazarakioti, K. M. Poole, L. Cunha-Silva, G. Christou and Th. C. Stamatatos, *Dalton Trans.*, 2014, **43**, 11456-11460.
- For examples of our previous work, see: (a) V. Bekiari, K. A. Thiakou, C. P. Raptopoulou, S. P. Perlepes and P. Lianos, *J. Lumin.*, 2008, **128**, 481; (b) H. Nikolaou, A. Terzis, C. P. Raptopoulou, V. Psycharis, V. Bekiari and S. P. Perlepes, *J. Surfaces Interfaces Mater.*, 2014, **2**, 311.
- N. S. Baek, Y. H. Kim, Y. K. Eom, J. H. Oh, H. K. Kim, A. Aebischer, F. Gumy, A.-S. Chauvin and J.-C. G. Bunzli, *Dalton Trans.*, 2010, **39**, 1532, and refs. cited therein.
- For reviews perspectives, see: (a) R. Sessoli and A. K. Powell, *Coord. Chem. Rev.*, 2009, **253**, 2328; (b) P. Zhang, Y.-N. Guo and J. Tang,

- Coord. Chem. Rev.*, 2013, **257**, 1728; (c) Y.-N. Guo, G.-F. Xu, Y. Guo and J. Tang, *Dalton Trans.*, 2011, **40**, 9953.
- 19 For example, see: (a) M. Yadav, V. Mereacre, S. Lebedkin, M. M. Kappes, A. K. Powell and P. W. Roesky, *Inorg. Chem.*, 2015, **54**, 773; (b) M. Fang, H. Zhao, A. V. Prosvirin, D. Pinkowicz, B. Zhao, P. Cheng, W. Wernsdorfer, E. K. Brechin and K. R. Dunbar, *Dalton Trans.*, 2013, **42**, 14693; (c) V. Chandrasekhar, S. Hossain, S. Das, S. Biswas and J.-P. Sutter, *Inorg. Chem.*, 2013, **52**, 6346; (d) F. Habib, J. Long, P.-H. Lin, I. Korobkov, L. Ungur, W. Wernsdorfer, L. F. Chibotaru and M. Murugesu, *Chem. Sci.*, 2012, **3**, 2158; (e) R. J. Blagg, L. Ungur, F. Tuna, J. Speak, P. Comar, D. Collison, W. Wernsdorfer, E. J. L. McInnes, L. F. Chibotaru and R. E. Winpenny, *Nature Chem.*, 2013, **5**, 673; (f) D. Prodius, F. Macaev, Y. Lan, G. Novitchi, S. Pogrebnoi, E. Stingaci, V. Mereacre, C. E. Anson and A. K. Powell, *Chem. Commun.*, 2013, **49**, 9215; (g) M. Ren, D. Pinkowicz, M. Yoon, K. Kim, L.-H. Zheng, B. K. Breedlove and M. Yamashita, *Inorg. Chem.*, 2013, **52**, 8342; (i) R. McLellan, M. A. Palacios, C. M. Beavers, S. J. Teat, E. K. Brechin and S. J. Dalgarno, *Chem. Commun.*, 2013, **49**, 9552; (j) E. Gavey, Y. Beldjoudi, J. M. Rawson, Th. C. Stamatatos and M. Pilkington, *Chem. Commun.*, 2014, **50**, 3741; (k) E. M. Fatila, M. Rouzieres, M. C. Jennings, A. J. Lough, R. Clérac and K. E. Preuss, *J. Am. Chem. Soc.*, 2013, **135**, 9596; (l) J. D. Rinehart, M. Fang, W. J. Evans and J. R. Long, *J. Am. Chem. Soc.*, 2011, **133**, 14236.
- 20 (a) F. Habib and M. Murugesu, *Chem. Soc. Rev.*, 2013, **42**, 3278; (b) E. Moreno Pineda, N. F. Chilton, R. Marx, M. Dörfel, D. O. Sells, P. Neugebauer, S.-D. Jiang, D. Collison, J. van Slageren, E. J. L. McInnes and R. E. P. Winpenny, *Nature Commun.*, 2014, **5**, 5243.
- 21 For an example from our group, see: A. Panagiotopoulos, Th. F. Zafiroopoulos, S. P. Perlepes, E. Bakalbassis, I. Masson-Ramade, O. Kahn, A. Terzis and C. P. Raptopoulou, *Inorg. Chem.*, 1995, **34**, 4918.
- 22 P.-H. Lin, T. J. Burchell, R. Clérac and M. Murugesu, *Angew. Chem. Int. Ed.*, 2008, **47**, 8848.
- 23 (a) A. B. Canaj, G. K. Tsikalas, A. Philippidis, A. Spyros and C. J. Milios, *Dalton Trans.*, 2014, **43**, 12486; (b) N. C. Anastasiadis, C. M. Granadeiro, N. Klouras, L. Cunha-Silva, C. P. Raptopoulou, V. Psycharis, V. Bekiari, S. S. Balula, A. Escuer and S. P. Perlepes, *Inorg. Chem.*, 2013, **52**, 4145.
- 24 For example, see: (a) S. Dutta, P. Basu and A. Chakravorty, *Inorg. Chem.*, 1991, **30**, 4031; (b) K. I. Alexopoulou, E. Zagoraiou, Th. F. Zafiroopoulos, C. P. Raptopoulou, V. Psycharis, A. Terzis and S. P. Perlepes, *Spectrochim. Acta, Part A*, 2015, **136**, 122.; (c) M. K. Koley, S. C. Sivasubramanian, B. Varghese, P. T. Manoharan and A. P. Koley, *Inorg. Chim. Acta*, 2008, **361**, 1485.
- 25 (a) D. I. Alexandropoulos, T. N. Nguyen, L. Cunha-Silva, Th. F. Zafiroopoulos, A. Escuer, G. Christou and Th. C. Stamatatos, *Inorg. Chem.*, 2013, **52**, 1179; (b) H. Wang, H. Ke, S.-Y. Lin, Y. Guo, L. Zhao, J. Tang and Y.-H. Li, *Dalton Trans.*, 2013, **42**, 5298.
- 26 S. Mukherjee, A. K. Chaudhuri, S. Xue, J. Tang and S. K. Ghosh, *Inorg. Chem. Commun.*, 2013, **35**, 144.
- 27 E. Labisbal, L. Rodriguez, A. Vizoso, M. Alonso, J. Romero, J.-A. Garcia-Vázquez, A. Sousa-Pedrares and A. Sousa, *Z. Anorg. Allg. Chem.*, 2005, **631**, 2107.
- 28 *CrystalClear*, Rigaku/MSI Inc., The Woodlands, TX, USA, 2005.
- 29 G. M. Sheldrick, *SHELXS-97: Structure Solving Program*, University of Göttingen, Germany, 1997.
- 30 G. M. Sheldrick, *SHELXL-97: Crystal Structure Refinement Program*, University of Göttingen, Germany, 1997.
- 31 Th. C. Stamatatos, G. S. Papaefstathiou, L. R. MacGillivray, A. Escuer, R. Vicente, E. Ruiz and S. P. Perlepes, *Inorg. Chem.*, 2007, **46**, 8843.
- 32 C. Airoldi, *Inorg. Chem.*, 1981, **20**, 998.
- 33 K. Nakamoto, *Infrared and Raman Spectra of Inorganic and Coordination Compounds*, Wiley, New York, 4th edn, 1986, pp. 254-257.
- 34 M. Llunell, D. Casanova, J. Girera, P. Alemany and S. Alvarez, *SHAPE, version 2.0*, Barcelona, Spain, 2010.
- 35 S. Alvarez, P. Alemany, D. Casanova, J. Girera, M. Llunell and D. Avnir, *Coord. Chem. Rev.*, 2005, **249**, 1693.
- 36 E. L. Muetterties and C. M. Wright, *Quart. Rev. Chem. Soc.*, 1967, **21**, 109.
- 37 (a) M. Nematirad, W. J. Gee, S. K. Langley, N. F. Chilton, B. Moubaraki, K. S. Murray and S. R. Batten, *Dalton Trans.*, 2012, **41**, 13711; (b) X. Yi, K. Bernot, O. Cador, J. Luzon, G. Calvez, C. Daiguebonne and O. Guillou, *Dalton Trans.*, 2013, **42**, 6728.
- 38 J. Long, F. Habib, P.-H. Lin, I. Korobkov, G. Enright, L. Ungur, W. Wernsdorfer, L. F. Chibotaru and M. Murugesu, *J. Am. Chem. Soc.*, 2011, **133**, 5319.
- 39 F. Cimoosu, F. Dahan, S. Ladeira, M. Ferbinteanu and J.-P. Costes, *Inorg. Chem.*, 2012, **51**, 11279.
- 40 We thank two referees who raised these points.
- 41 (a) Y.-N. Guo, G.-F. Xu, W. Wernsdorfer, L. Ungur, Y. Guo, J. Tang, H.-J. Zhang, L. F. Chibotaru and A. K. Powell, *J. Am. Chem. Soc.*, 2011, **133**, 11948; (b) K. Katoh, Y. Horii, N. Yasuda, W. Wernsdorfer, K. Toriumi, B. K. Breedlove and M. Yamashita, *Dalton Trans.*, 2012, **41**, 13582.
- 42 K. C. Mondal, A. Sundt, Y. Lan, G. E. Kostakis, O. Waldmann, L. Ungur, L. F. Chibotaru, C. E. Anson and A. K. Powell, *Angew. Chem., Int. Ed.*, 2012, **51**, 7550.
- 43 P. -E. Car, M. Perfetti, M. Mannini, A. Favre, A. Caneschi and R. Sessoli, *Chem. Commun.*, 2011, **47**, 3751.
- 44 N. F. Chilton, D. Collison, E. J. L. McInnes, R. E. P. Winpenny and A. Soncini, *Nature Commun.*, 2013, **4**, 2551.
- 45 D. J. Newman and B. K. C. Ng, *Crystal Field Handbook*, Cambridge University Press, Cambridge, UK, 2000.
- 46 J.-C. G. Bünzli and C. Piguet, *Chem. Soc. Rev.*, 2005, **34**, 1048.
- 47 (a) D. Sykes, A. J. Cankut, N. M. Ali, A. Stephenson, S. J. P. Spall, S. C. Parker, J. A. Weinstein and M. Ward, *Dalton Trans.*, 2014, **43**, 6414; (b) N. M. Shavaleev, Z. R. Bell and M. D. Ward, *J. Chem. Soc., Dalton Trans.*, 2002, 3925.

GRAPHICAL ABSTRACT

The bridging potency of the dianionic form of *N*-salicylidene-*o*-aminophenol has been exploited for the preparation of dinuclear lanthanide(III) complexes; the Dy^{III}₂ complex is bifunctional exhibiting both photoluminescence and slow relaxation of its magnetization.

